UNICA UNIVERSITÀ DEGLI STUDI DI CAGLIARI

This is the Author's *accepted* manuscript version of the following contribution:

Araceli Guadalupe Romero-Izquierdo, Fernando Israel Gómez-Castro, Claudia Gutiérrez-Antonio, Salvador Hernández, Massimiliano Errico,

Intensification of the alcohol-to-jet process to produce renewable aviation fuel, Chemical Engineering and Processing - Process Intensification, Volume 160, 2021, 108270.

© <2020>. This manuscript version is made available under the CC-BY-NC-ND 4.0 license https://creativecommons.org/licenses/by-nc-nd/4.0/

The publisher's version is available at:

http://dx.doi.org/10.1016/j.cep.2020.108270

When citing, please refer to the published version.

This full text was downloaded from UNICA IRIS https://iris.unica.it/

Intensification of the alcohol-to-jet process to produce renewable aviation fuel

Araceli Guadalupe Romero-Izquierdo [a], Fernando Israel Gómez-Castro [a,*], Claudia Gutiérrez-Antonio [b], Salvador Hernández [a], Massimiliano Errico [c]

[a] *Departamento de Ingeniería Química, División de Ciencias Naturales y Exactas, Campus Guanajuato, Universidad de Guanajuato, Noria Alta S/N, Col. Noria Alta, Guanajuato, Guanajuato, 36050, México.*

[b] *Universidad Autónoma de Querétaro, Facultad de Química, Cerro de las Campanas s/n Col. Las Campanas, Querétaro, Querétaro, 76010, México.*

[c] *University of Southern Denmark, Faculty of Engineering, Department of Green Technology, Campusvej 55, 5230 Odense M, Denmark.*

Abstract

The biojet fuel production has been considered a promising strategy to partially satisfy the aviation fuel demand. Recently, the biojet fuel obtained from the alcohol-to-jet (ATJ) process has been certified by the American Society of Testing Materials (ASTM). In this work, the modelling and simulation of the ATJ conventional process is presented, considering as raw material bioethanol produced from lignocellulosic wastes. To reduce the energy requirements and the environmental impact, process intensification tools are applied on the separation zone, followed by the energy integration of the whole process. The ATJ conventional and intensified-integrated processes are assessed by the total annual cost (TAC) and the CO_2 emissions. According to the results, the intensification on the separation zone allows reducing energy requirements by 5.31% in contrast to the conventional sequence; moreover, the energy integration of the intensified process reduces by 34.75% and 30.32% the heating and cooling requirements, respectively; as consequence, TAC and CO_2 emissions are decreased by 4.83% and 4.99%, respectively, when compared to the conventional

process. Nevertheless, the electricity generated by the turbines completely satisfies the electrical energy requirement of the process.

Keywords: renewable aviation fuel, alcohol-to-jet, process intensification, energy integration.

* Author to whom all correspondence should be addressed, e-mail: fgomez@ugto.mx, phone: (52) 473 73 20006 ext. 1406.

1. Introduction

Worldwide, the energy demand is a priority theme. According to BP [1], the estimated energy requirement for 2040 will be 25% more than the amount required in 2019.

With this trend the estimated increase of CO2 emissions can reach an alarming 10% increase by the same year. Considering that most of the energy is produced from non-renewable sources, it is necessary to increase the production of sustainable energy, in order to reduce the environmental impacts. In particular, the transport sector is one the major player in the energetic transition since it consumes 21% of world energy demand, and the forecast indicates an increase up to 130% by 2050 [1]. Among the means of transport, the aviation industry has the major growth rate; it is estimated that it will duplicate its jet fuel consumption in the next 20 years, increasing correspondingly its CO_2 emissions [2]. Martínez-Hernández et al. [3], estimated that in 2050 the CO_2 emissions from aviation sector will increase 300-700%, compared to 2005, if no changes on the current technologies and the flight patterns occur. Nevertheless, the actual world pandemic caused by COVID-19 has changed all economic sectors; in the aviation industry the losses are estimated in 16 billion dollars for 2021 [4]. Also, the International Air Transport Association (IATA) indicates that the new social distancing measures caused a reduction of the load factor to 62%. [5]. Thereby, compared to 2019, the air fares of airlines increased between 43% and 54%, depending on the region of the world. More than ever, it is necessary to focus on the sustainable recovery of the aviation sector, with novel strategies to mitigate the crisis; keeping at the same time ambitious objectives such as 50% reduction in CO_2 emissions by 2050, compared to 2005 levels [6, 7]. To achieve these goals, a four-pillar strategy has been proposed, including: 1) technological improvements in engines and aircrafts, 2) operational improvements by optimization of flight paths, 3) market-based actions, and 4) development of alternative fuels [6]. In particular, the development of alternative fuels has been identified as the most promising strategy to reduce the environmental impact in the short and medium-term reaching also a partial independence from non-renewable sources [6, 8]. The renewable aviation fuel, also called

biojet fuel or synthetic paraffinic kerosene (SPK), is a mixture of renewable hydrocarbons in the boiling range of fossil jet fuel. Its chemical composition and properties are similar to that of fossil jet fuel, being the main difference the content of aromatic compounds [6, 8-9]. The absence of such compounds can cause sealing issues in certain types of engines [10]; because of that, it is used in mixtures with a maximum of biojet fuel of 50% in volume [11]. This alternative fuel can be produced from triglyceride, lignocellulosic, sugars and starchy biomasses, which can be edible, non-edible and wastes [12]. Depending on the selected feedstock, there are six conversion routes to produce biojet fuel certified by ASTM: Fischer-Tropsch (FT-SPK), Hydroprocessed Esters and Fatty Acids (HEFA-SKP), Direct Sugars to Hydrocarbons (DSC), Fisher-Tropsch with Aromatics (FT-SPK/A), Alcohol to Jet (ATJ-SPK) and Co-processing of renewable lipids with crude oil-derived middle distillates [12]. HEFA and DSC are in commercialization stage, while FT-SPK, FT-SPK/A and ATJ-SPK are in demonstration levels. However, the biojet fuel produced by any of these processes is not economically competitive [13]; it is important to apply strategies to reduce the energy requirements and the size of the equipment on the production processes, to achieve the economic and environmental sustainability of biojet fuel.

Among all the production processes, one of the most recent is ATJ, which obtained the certification of American Society of Testing Materials (ASTM) in 2016 [13]. The ATJ process uses as raw material bio-alcohols, such as methanol, ethanol, butanol and long chain fatty alcohols, priorly produced from starch, sugars, and lignocellulosic feedstocks [14]. This process involves three reactive stages: dehydration of alcohol, oligomerization and hydrogenation, along with the separation stage to purify naphtha, biojet fuel and green diesel (Figure 1). The biojet fuel produced by the ATJ process can be used in mixtures with fossil jet fuel with up to 50 vol% of bio-jet fuel, according to the ASTM D7566 standard [15, 16]. The main advantage of this process is that each stage has been commercially demonstrated, as part from other processes, minimizing the risk of scaling-up of the whole ATJ process [14]. On the other hand, due to the low yield and conversion associated with the alcohol

production from biomass, the raw material price of ATJ process could increase. Thus, it is necessary to increase the bio-alcohols production efficiency in order to improve the economic and environmental sustainability of the ATJ process. However, it is important to remark that, even if the alcohol production is a critical stage, it is out of the ATJ processing. A compilation of reports about each conversion stage involved in the ATJ process is focused mainly on the proposal of novel catalysts to improve the yield and conversion of each reactive system [2, 14]. Among them, few works have reported the modelling and analysis of the complete ATJ process. In 2015, Atsonios et al. [17] studied the production of biojet fuel through three simultaneous processes to convert the lignocellulosic biomass into alcohol: gasification, Fischer-Tropsch and biochemical pathways; in addition, they made an economic comparison between all the processes, which were modelled in Aspen Plus. The conversion of n-butanol and isobutanol into biojet fuel was realized through the ATJ process. According to the results, the minimum selling price is obtained with the FT process. Later, the techno-economic analysis of ATJ process was presented, using bioethanol from corn grain and corn stover concluding that biojet fuel could be economically competitive if the yield of sugar to ethanol is increased [18]. In 2018, Neuling and Kaltschmith [19] presented a comparison between four different production processes to obtain biojet fuel from lignocellulosic materials and grains, including the ATJ process. Their results exhibited that the ATJ process using wheat grain as feedstock is the best option, in economic and environmental terms. Recently, a report about the integration of pulp mill operation with ATJ process was presented, analyzing the feasibility of a biorefinery scheme [20]. According to the results, the integration of ATJ process into pulp mill operation could reduce the processing cost of biojet fuel. It is important to mention that all reports described before present the ATJ process in the conventional form (Figure 1), proving its technical efficiency regarding to other biojet fuel processes; however, the application of strategies to reduce its energy consumption, that allows to achieve the economic competitiveness of biojet fuel, represents an area of opportunity which has not been explored in detail.

Process intensification and energy integration are two important tools that have proved to reduce the energy consumption of the processes. There are some reports focused on the use of intensification techniques with energy integration applied on distillation columns; as a result, novel configurations are proposed such as heat-pump distillation, heat-integrated distillation, dividing wall column, vapor recompression column, among others [21]. Gao et al. [22] reported a configuration of reactive distillation with heat-integrated to synthetize tert-amyl methyl ether (TAME); this configuration was compared with a conventional reactive column, demonstrating economic and energetic savings. Cong et al. [23] proposed a multi-tube heat integrated distillation column to separate binary mixtures; they found that this design improves the operational flexibility from the system, allowing important energy and economic savings. Regarding the operational flexibility, Cong et al. [24] reported a novel middle vapor recompression distillation column, based on a heat-integrated distillation column to increase both the energy savings and the profit. According to their analysis, this configuration allows a wide range of applications due to its operational flexibility, regarding to the basic heat-integrated distillation column and the vapor recompression column. Thus, to increase the recovery of waste heat, a Rankine cycle was integrated with an economizer in the operation of an extractive distillate system, to separate the azeotropic mixture n-heptane/isobutanol [25]. The results indicated that the use of this novel system allows saving up to 30.30% of TAC, and 45% of hot utility consumption. On the other hand, the application of intensified distillation sequences to separate biojet fuel has been reported in a few works. In 2015, Gutiérrez-Antonio et al. [26] proposed the intensification of a hydrotreating process to produce biojet fuel using thermally coupled distillation sequences, which include direct and indirect conventional distillation columns, the Petlyuk column and the dividing wall column. All the proposed sequences were optimized by a multi-objective genetic algorithm coupled to Aspen Plus. Based on the results, the direct thermally coupled sequence reached the major energy savings. In 2016, the application of energy integration and process intensification tools for the hydrotreating process to produce biojet fuel using *Jatropha curcas* oil was proposed [8]. The intensification was applied on the separation zone, analyzing two conventional sequences and two thermally coupled

schemes; both were optimized by a multiobjective genetic algorithm with constraints handling. The results of the economic and environmental assessment show that the process including the direct conventional distillation sequence with energy-integration had the major savings. Regarding the use of reactive distillation schemes, in 2018 the use of a reactive distillation column to produce biojet fuel was reported [27]. The results indicated that the use of reactive distillation allows decreasing the operation pressure, increasing the yield of biojet fuel and improving the environmental impact. The use of conventional and intensified distillation sequences for the hydroprocessing of microalgae oil has also been reported [28]. The conclusions of the study show that the implementation of the intensified distillation sequences allowed a decrease of 34 % of the CO_2 emissions and the improvement of the biojet fuel price. A brief review of intensification strategies applied to the production of renewable jet fuel is presented by Gutiérrez-Antonio et al. [29]. In addition, an intensified three-step reaction-separation process to produce aviation fuel from a mixture of triglycerides and petro-diesel was proposed in 2019 [30], through an hydrolysis section and a reactive hydrodesulphurization and hydrodeoxygenation reactive distillation column (HDS-HDO); this study determined that optimal operating conditions to produce the biojet fuel are 553 K for hydrolysis, with 14 stages and 30 atm of pressure for the HDS-HDO reactive column.

On the other hand, the energy integration tool has been applied on the complete hydrotreating process adding the intensification on separation stage [6], as well as in two processes to produce renewable fuels into a biorefinery scheme [31]. In each one of these reports, the energy consumption has been reduced, and the CO_2 emissions related to these processes are lower than those for conventional processes. Thus, in this work the modelling and simulation of the ATJ process is presented, using bioethanol produced from lignocellulosic wastes as raw material; moreover, process intensification tools are applied on the separation zone of ATJ. Later, the ATJ process with the intensified sequence of minor energy consumption is improved through the application of the energy integration. Both ATJ processes, conventional and intensified-integrated, are evaluated using the total annual cost and

the CO_2 emissions, as main performance indicators. It is important to remark that the bioethanol production process is not considered in this study.

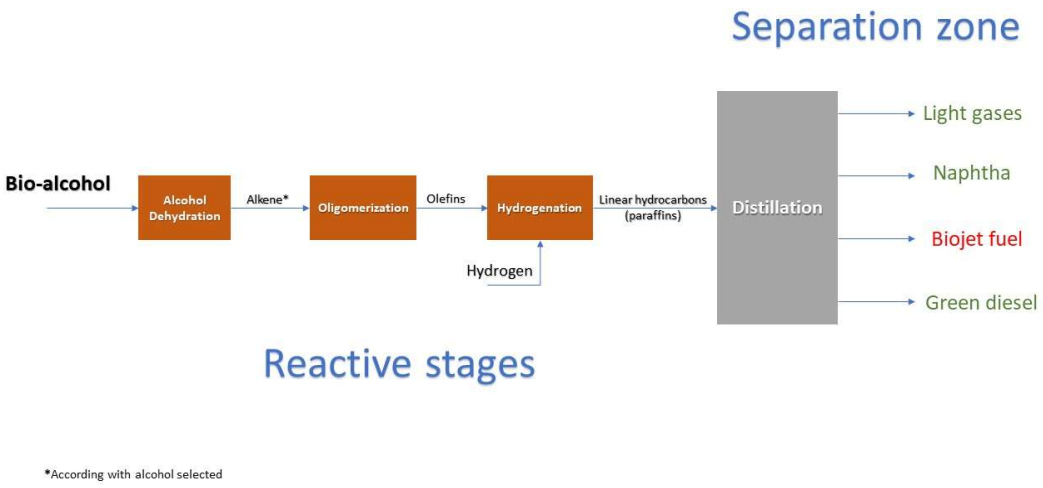

Figure 1. Block diagram of conventional ATJ process.

2. Modelling of ATJ process

The feedstock of the ATJ process is the effluent from the co-fermentation reactor, reported by Conde-Mejía et al [32], which is part of the bioethanol production process with lignocellulosic wastes as raw material. This effluent is formed by 257,673 kg/h of bioethanol, with traces of glycerol, water, and ammonia. The ATJ process involves three reactive stages: dehydration, oligomerization and hydrogenation, and a separation zone. In the first reactive stage, the bioethanol is dehydrated at 450 °C and 11.4 bar, adding saturated steam to reach 99.5% of ethylene conversion. The operating conditions and the conversion data (see Table 1) were extracted from the work of Lundin [33]. In Aspen Plus, this reactive stage is modelled by the RStoic module, using the reactions presented in Table 1. The obtained ethylene from this reactive stage is fed to a turbine, diminishing the stream pressure until 3 bar. This pressure condition is necessary to separate the ethylene in a distillation

column, represented by a RadFrac module, with partial vapor-liquid condenser, designed to recover 99% of ethylene.

Table 1. Dehydration reactions and conversion data. Extracted from [33].

Reactions	Conversion	Reference reactive
$C_2H_6O \rightarrow C_2H_4 + H_2O$	0.988	
$2\,C_2H_6O \rightarrow (C_2H_5)_2O + H_2O$	0.00052	Ethanol
$C_2H_6O \rightarrow (C_2H_4O) + H_2$	0.002	

The recovered ethylene is fed to the second reactive stage, i.e. oligomerization; this stage operates at 120 °C and 35 bar. In Aspen Plus, this reactor is modelled with the RStoic module, using the reactions set shown in Table 2, with the conversion data reported by Heveling et al. [34]. The oligomerized products are fed to the third reactive stage, which is operated at 100 °C and 15 bar of hydrogen [35], achieving until 99% of conversion to paraffins. In Aspen Plus, this reactive stage is modelled by RStoic module, using the reactions presented in Table 3.

Table 2. Oligomerization reactions and conversion data. Extracted from [34].

Reactions	Conversion	Reference reactant
$2C_2H_4 \rightarrow C_4H_8$	0.32	
$2.5C_2H_4 \rightarrow C_5H_{10}$	0.0015	
$3C_2H_4 \rightarrow C_6H_{12}$	0.24	
$3.5C_2H_4 \rightarrow C_7H_{14}$	0.0015	
$4C_2H_4 \rightarrow C_8H_{16}$	0.18	
$4.5C_2H_4 \rightarrow C_9H_{18}$	0.0015	

$5C_2H_4 \rightarrow C_{10}H_{20}$	0.043	
$5.5C_2H_4 \rightarrow C_{11}H_{22}$	0.0015	Ethylene
$6C_2H_4 \rightarrow C_{12}H_{24}$	0.043	
$7C_2H_4 \rightarrow C_{14}H_{28}$	0.043	
$7.5C_2H_4 \rightarrow C_{15}H_{30}$	0.0015	
$8C_2H_4 \rightarrow C_{16}H_{32}$	0.043	
$8.5C_2H_4 \rightarrow C_{17}H_{34}$	0.0015	
$9C_2H_4 \rightarrow C_{18}H_{36}$	0.043	
$9.5C_2H_4 \rightarrow C_{19}H_{38}$	0.0015	
$10C_2H_4 \rightarrow C_{20}H_{40}$	0.043	

Table 3. Hydrogenation reactions and conversion data [35].

Reactions	**Conversion**	**Reference reactant**
$C_4H_8 + H_2 \rightarrow C_4H_{10}$		n-Butene
$C_5H_{10} + H_2 \rightarrow C_5H_{12}$		n-Pentene
$C_6H_{12} + H_2 \rightarrow C_6H_{14}$		n-Hexene
$C_7H_{14} + H_2 \rightarrow C_7H_{16}$		n-Heptene
$C_8H_{16} + H_2 \rightarrow C_8H_{18}$		n-Octene
$C_9H_{18} + H_2 \rightarrow C_9H_{20}$		n-Nonene
$C_{10}H_{20} + H_2 \rightarrow C_{10}H_{22}$		n-Decene
$C_{11}H_{22} + H_2 \rightarrow C_{11}H_{24}$	0.99	n-Undecene
$C_{12}H_{24} + H_2 \rightarrow C_{12}H_{26}$		n-Dodecene
$C_{14}H_{28} + H_2 \rightarrow C_{14}H_{30}$		n-Tetradecene
$C_{15}H_{30} + H_2 \rightarrow C_{15}H_{32}$		n-Pentadecene
$C_{16}H_{32} + H_2 \rightarrow C_{16}H_{34}$		n-Hexadecene

$C_{17}H_{34} + H_2 \rightarrow C_{17}H_{36}$	n-Heptadecene
$C_{18}H_{36} + H_2 \rightarrow C_{18}H_{38}$	n-Octadecene
$C_{19}H_{38} + H_2 \rightarrow C_{19}H_{40}$	n-Nonadecene
$C_{20}H_{40} + H_2 \rightarrow C_{20}H_{42}$	n-Eicosene

The renewable hydrocarbons from the last reactive stage enter to a turbine to decrease its pressure until 1 bar, before its fed to the separation zone. In Table 4 the component distribution of renewable hydrocarbons is showed.

Table 4. Product distribution from the third reactive stage.

Compounds distribution	**kg/h**	**Products**
n-Butene	482.59	
n-Butane	49492.8	Light gases (A)
n-Pentene	2.28	
n-Pentane	232.35	
n-Hexane	36175.4	Naphtha (B)
n-Hexene	356.86	
n-Heptene	2.28	
n-Heptane	230.50	
n-Octene	272.94	
n-Octane	27506.9	
n-Nonene	2.28	
n-Nonane	229.47	
n-Decane	6473.38	
n-Undecane	228.81	
n-Decene	64.46	

n-Dodecene	64.46	Biojet fuel (C)
n-Dodecane	6458.10	
n-Undecene	2.28	
n-Tetradecene	64.46	
n-Tetradecane	6447.18	
n-Pentadecane	228.03	
n-Hexadecene	64.30	
n-Pentadecene	2.28	
n-Hexadecane	6374.60	
n-Heptadecane	2.28	
n-Octadecene	0.0021	
n-Octadecane	0.18	
n-Nonadecane	0.0062	Green diesel (D)
n-Eicosane	0.18	
n-Nonadecene	6.36E-05	
n-Eicosene	0.0018	

As it can be seen, there are four pseudo-components to separate; thus, a distillation train with three columns is designed in Aspen Plus using short cut methods (DSTWU module), and later this design is rigorously simulated through RadFrac module [26]. The first distillation column has a partial-vapor condenser to separate the light gases at the top, using the 314-A refrigerant as cooling medium; the bottom of this column is the feed stream to the second one, wherein the naphtha cut is separated at the top while its bottom stream enters to a third distillation column. This last column separates biojet fuel at the top, whilst green diesel is obtained at the bottom. The number of stages in each column are 16, 33 and 87, respectively; this design is called direct conventional. In Figure 2 the ATJ process described before is shown. The thermodynamic model used to simulate this process was Peng-

Robinson, except the distillation train, whose phase equilibrium was modelled using the BK10 model [36].

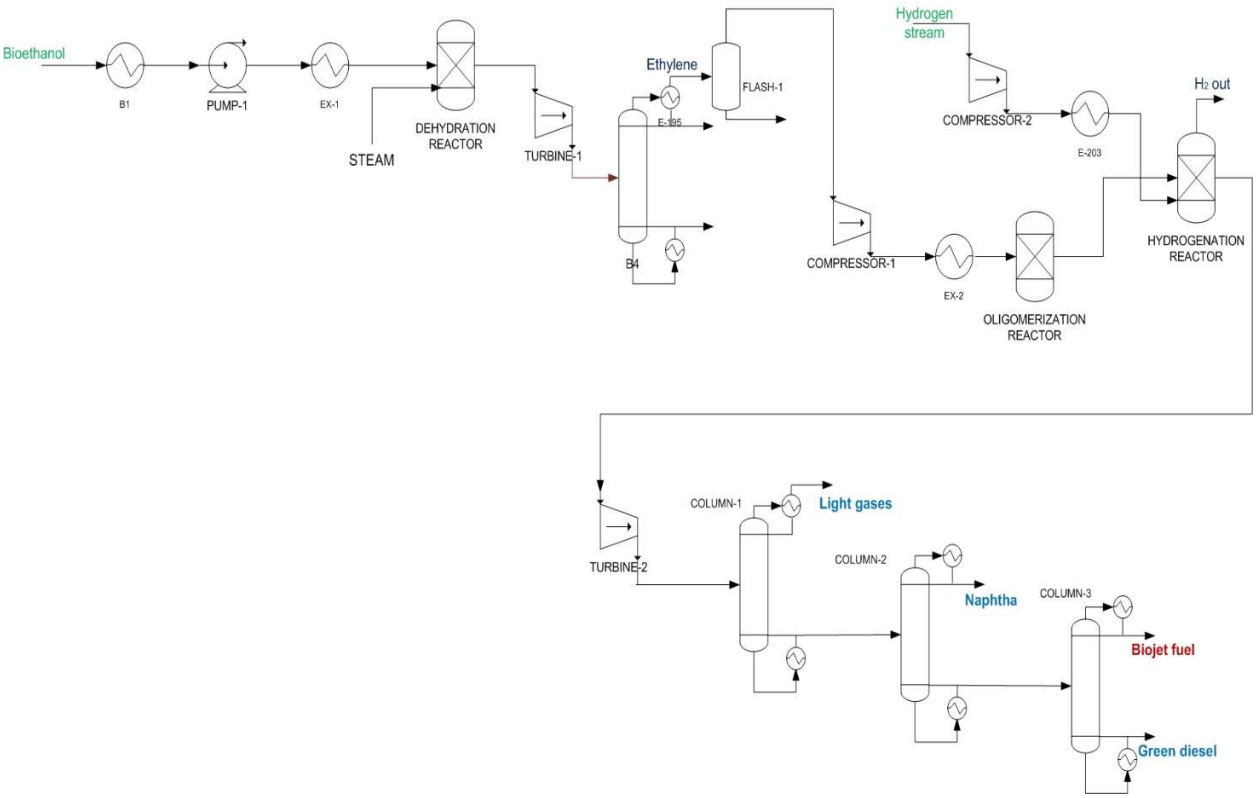

Figure 2. Flowsheet of ATJ conventional process.

3. Process intensification: separation zone

Based on the product distribution and the direct conventional design, other distillation sequences with lower energetic consumption can be proposed using process intensification tools. In this work, the intensified sequences will be designed using the methodology proposed by Rong and Errico [37]. This methodology is schematically represented by the next steps:

Step 1. Create the subspace of simple column configurations (SC).

Step 2. Select the simple column configuration with less energy consumption, from the previous subspace.

Step 3. Generate the original thermally coupled configurations, replacing systematically reboilers or condensers (OTC), and select the OTC with less energy consumption.

Step 4. Generate the thermodynamically equivalent structures (TES) from OTC´s, using the sections re-arrangement methodology.

Step 5. Identify the TES´s that contain columns with a unique lateral transport section, keeping the structure of simple columns; then, the TES with less energy consumption is selected.

Step 6. Generate the intensified configurations (ISC) by eliminating the lateral transport section in the identified TES.

Step 7. If you do not select the structure with less energy consumption in steps 2 to 6, repeat these steps until all simple column configurations have been examined.

Step 8. Summarize all the ISC configurations.

It is important to mention that the light gases must be separated in the first distillation column, due to their low boiling point. Thus, in this work all generated sequences will have a fixed distillation column with partial-vapor condenser for the separation of light gases using the 314-A refrigerant, while the methodology described before is applied for the other distillation columns of the train. Likewise, in each step of this methodology the sequences will be evaluated, selecting the train with less energy consumption in each case. At the end, the sequence with the lowest energetic requirements will be selected as the distillation train from ATJ process.

4. Energy integration

According to the modelling of reactive stages and considering the distillation sequence with the lowest energy requirements obtained by following the methodology presented in Section 3, the ATJ process can be energetically integrated. The simulation in Aspen Plus allows knowing the data from energy and material balances for the complete process. This information is used to minimize the external utilities, integrating the available energy from the whole process through the Pinch point methodology. This methodology is well-known to reach various objectives, mainly the heat recovery, minimization of saturated steam and fresh water and minimization of the heat exchangers used [38]. The steps for the pinch point methodology are:

Step 1. Summarize temperatures, flowrates, and enthalpies of all process streams. This data can be obtained from Aspen Plus. The streams are classified as hot or cold streams.

Step 2. Definition of minimum difference of temperature. The streams are adjusted with the minimum difference: Hot steams – ΔT, and Cold streams without change.

Step 3. Definition of temperature intervals, considering the adjusted streams from Step 2. In each defined interval the energy balance is applied.

Step 4. Construction of the heat cascade based on the energy balances from Step 3. The cascade allows obtaining the pinch point.

Step 5. Construction of the heat exchanger network, taking account of the minimum number of heat exchangers, which are obtained above and below of pinch point. The minimum number of heat exchangers are calculated as:

$$\#\text{heat exchangers: } \#\text{ hot streams} + \#\text{ cold streams} + \text{utilities} - 1 \quad (1)$$

The heat cascade allows determining the heating and cooling utilities that cannot be fulfilled into the process. Thus, these energy requirements must be externally provided by steam or cooling water.

5. Economic and environmental assessment: parametric evaluation

The ATJ processes, conventional and the intensified-energetically integrated, are evaluated considering economic and environmental indicators. The economic evaluation is carried out by the calculation of total annual cost (TAC), defined as:

$$TAC\ (USD/year) = \frac{CC}{n} + OC \quad (2)$$

Where *CC* is the capital cost, which is associated with total equipment cost, estimated by Aspen Economics tool, *n* is the payback period, assumed as 5 years [39-41]. It has been assumed that the process operates 8,500 hours per year [8]. In accordance to Guthrie´s method, 18% is added to the cost obtained from Aspen Plus to include contingencies and other fees (regarding to installation cost). Similarly, 61% is added regarding to costs related with machinery, equipment and maintenance [39]. On the other hand, the operating cost (*OC*) is assumed as the sum of steam cost, cooling water, refrigerant (314-A), bioethanol, hydrogen, and electricity; all of them are required by the process and computed by the simulation software. In Table 5 are summarized the unitary cost of all utilities and reactants mentioned before.

Table 5. Summarized prices for operating cost.

Item	Price	Reference
Steam	1 USD/GJ	[42]
Cooling water	14.8 USD/1000 m^3	[39]
Refrigerant (R314A)	7.76 USD/kg	[43]
Ethanol	0.92 USD/L	[44]
Hydrogen	1.80 USD/kg	[45]
Electricity	1.4721 MX/kWh	[46]

Regarding the environmental evaluation, the estimation of CO_2 emissions considers those derived from the generation of steam and electricity, as external utilities, required by the process. The CO_2 emissions by steam generation are calculated through the methodology presented in [8], which takes into account the mass of burned fuel (gas natural) to fulfill the steam requirement, along with an emission factor due to combustion. In the case of CO_2 emissions due to the electricity generation, the emissions factor provided by the national electric system (Mexico) is used, which has a value of 0.582 ton of CO_2 per MWh [47]. It is important to mention that the emissions related with the 314-A refrigerant are not considered in this study.

According to Curzons et al. [48], different ratios between mass and energy from a process can be defined as indicators; they allow to measure its sustainability degree, analyzing the opportunity areas to minimize its energy consumption, improve the process efficiency, and minimize the released emissions. The comparison between processes using such defined indicators can be a tool for decision-making. In this work two indicators have been defined to analyze and compare both ATJ processes. The proposed indicators are presented next:

Indicator 1: Energetic indicator (IE).

The energetic indicator is defined as the ratio between the invested (required) energy for heating, regarding to the energy provided by the products, Eq. 3. The invested energy for heating is the total required energy for heating inside the process, whilst the provided energy is the sum of calorific value of each product multiplied by its production volume.

$$IE = \frac{Invested\ energy\ for\ heating}{Provided\ energy\ by\ the\ products} \tag{3}$$

Indicator 2: CO_2 emissions indicator (IACO2).

The CO_2 emissions indicator is defined as the relation between the total CO_2 equivalent emissions (provided by steam and electricity), regarding to total mass of the products. The total CO_2 emissions are obtained in the environmental evaluation mentioned before. This indicator is calculated through Eq. 4.

$$IACO2 = \frac{Total\ CO_2\ equivalent\ emissions}{Total\ mass\ of\ the\ products} \quad (4)$$

6. Analysis of results

In this section, the results obtained in this work are presented and discussed. According to the modelling and simulation of the ATJ process, 21% biojet fuel yield was obtained at the end of the reactive stages; this value is better than that reported by Tao et al. [18], wherein 16.90% and 10.70% of biojet fuel yield is obtained, respectively. It is important to mention that in Tao et al. [18], the biojet fuel yield was estimated taking into account the corn grain and corn stover as feedstocks. On the other hand, the hydrocarbon stream contains light gases (A, 49,782.8 kg/h), naphtha (B, 37,249.5 kg/h), biojet fuel (C, 54,429 kg/h) and green diesel (D, 13,511.1 kg/h), and their compounds distribution is presented in Table 4. Thus, only two simple distillation schemes can be designed: direct and combined. Also, it is important to remind that for all trains, at the top of the first distillation column the light gases are obtained using a partial-vapor condenser. These simple columns are designed using RadFrac modules in Aspen Plus (see the end of Section 2). The simple column configurations are presented in Figure 3, whilst its results from Aspen Plus are showed in Table 6. As it can be seen, the indirect scheme has 69 more stages than direct one; likewise, the combined configuration has 3.16% and 15.73% more cooling and heating requirements at condenser and reboiler, respectively. Thus, the direct scheme is chosen as basis to design the OTC´s sequences.

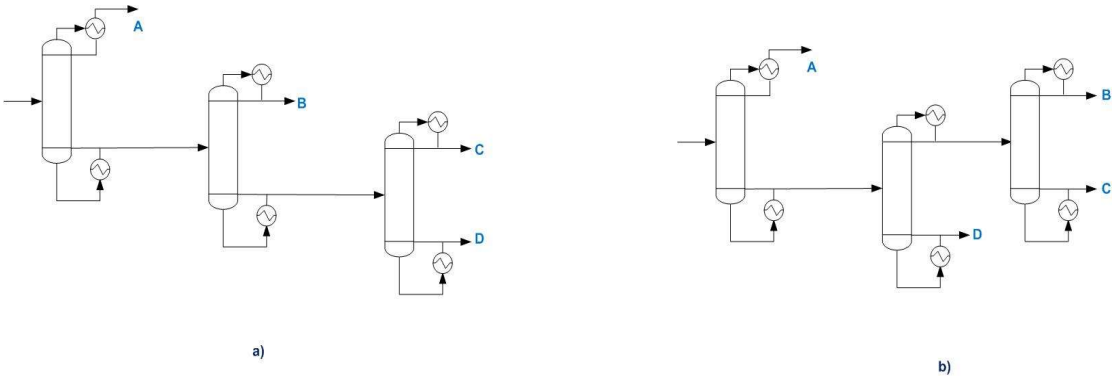

Figure 3. Simple column configurations: a) direct, b) combined.

Table 6. Results of direct and combined simple column configurations.

Direct simple column configuration				
	Column 1	**Column 2**	**Column 3**	**TOTAL**
Number of stages	16	33	87	136
Feed stage number	8	17	44	
Condenser duty (kW)	5,491.42	6,719.47	9,650.87	22,311.76
Reboiler duty (kW)	8,511.91	8,507.72	10,603.50	27,623.17
Combined simple column configuration				
	Column 1	**Column 2**	**Column 3**	**TOTAL**
Number of stages	16	155	34	205
Feed stage number	8	78	17	
Condenser duty (kW)	5,491.42	12,012.95	5,534.5	23,038.87
Reboiler duty (kW)	8,511.91	16,165.20	8,100.63	32,777.74

Based on the direct simple column configuration, three OTC´s sequences are designed (Figure 4); in each sequence, the reboilers are replaced by interconnecting flows. In Aspen Plus, these designs were simulated using Radfrac module, taking as basis the results presented in Table 6. The design variables of the resulting OTC´s are presented in Table 7.

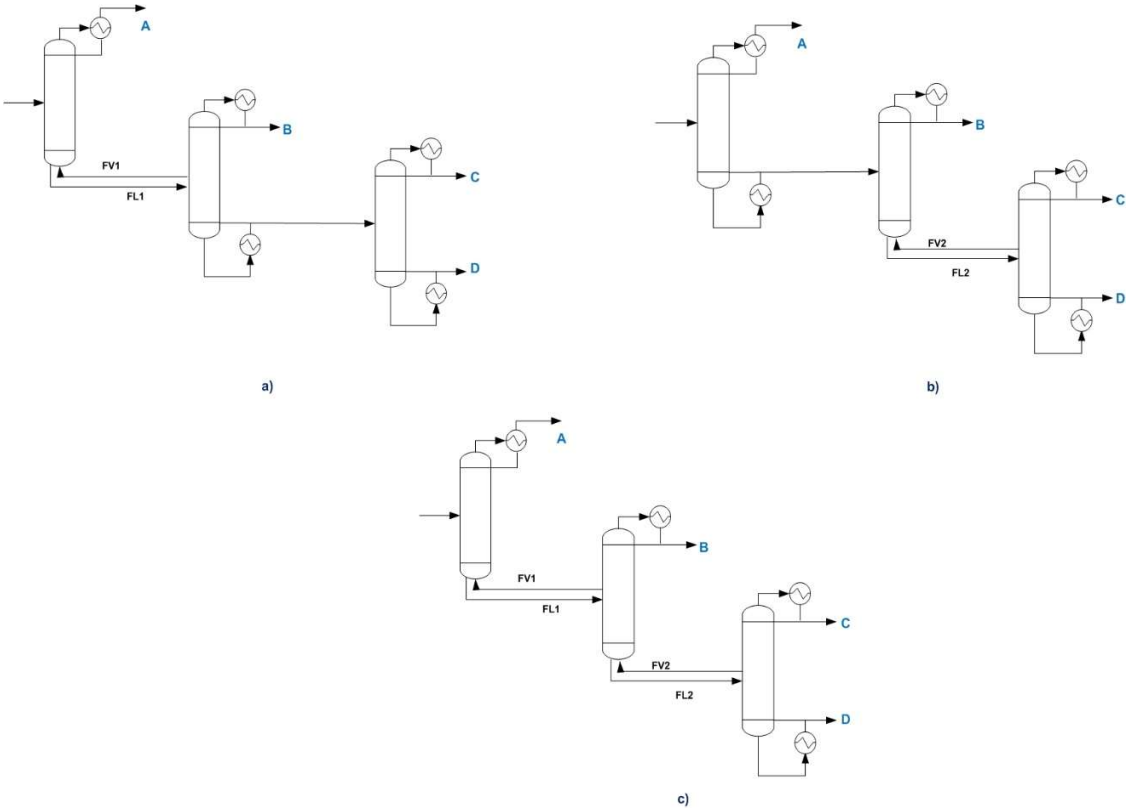

Figure 4. OTC´s configurations: a) OTC-1, b) OTC-2, c) OTC-3.

Table 7. Design variables of the OTC´s configurations.

	OTC-1			
	Column 1	**Column 2**	**Column 3**	**TOTAL**
Number of stages	16	33	87	136
Feed stage number	8	17	44	

Condenser duty (kW)	4,741.45	6,693.07	9,650.92	21,085.43
Reboiler duty (kW)	0	15.871.98	10,526.62	26,398.61
FV (kg/h)	75,803.3	**FL (kg/h)**		180,993
		OTC-2		
	Column 1	**Column 2**	**Column 3**	**TOTAL**
Number of stages	16	33	87	136
Feed stage number	8	17	44	
Condenser duty (kW)	5,491.42	9,112.79	9,650.88	24,705.09
Reboiler duty (kW)	8,511.91	0	21,506.50	30,018.41
FV (kg/h)	87,111,7	**FL (kg/h)**		155,052
		OTC-3		
	Column 1	**Column 2**	**Column 3**	**TOTAL**
Number of stages	16	33	87	136
Feed stage number	8	17	44	
Condenser duty (kW)	5,889.79	4,888.64	10,064.52	20,842.95
Reboiler Duty (kW)	0	0	26,156.65	26,156.65
FV-1 (kg/h)	89,808	**FL-1 (kg/h)**		194,998
FV-2 (kg/h)	12,000	**FL-2 (kg/h)**		187,940

From Table 7 it can be observed that the OTC-3 is the best sequence regarding to energy consumption, since its condenser duty is 1.15% and 15.63% less than OTC-1 and OTC-2, respectively. Likewise, the reboiler duty is 0.91% and 12.86% less than OTC-1 and OTC-2, respectively. Therefore, OTC-3 is chosen as basis to design the TES´s.

The TES´s are designed through the section re-arrangement methodology. In Figure 5, the three TES´s designed are shown, while in Table 8 its main results from Aspen Plus are presented.

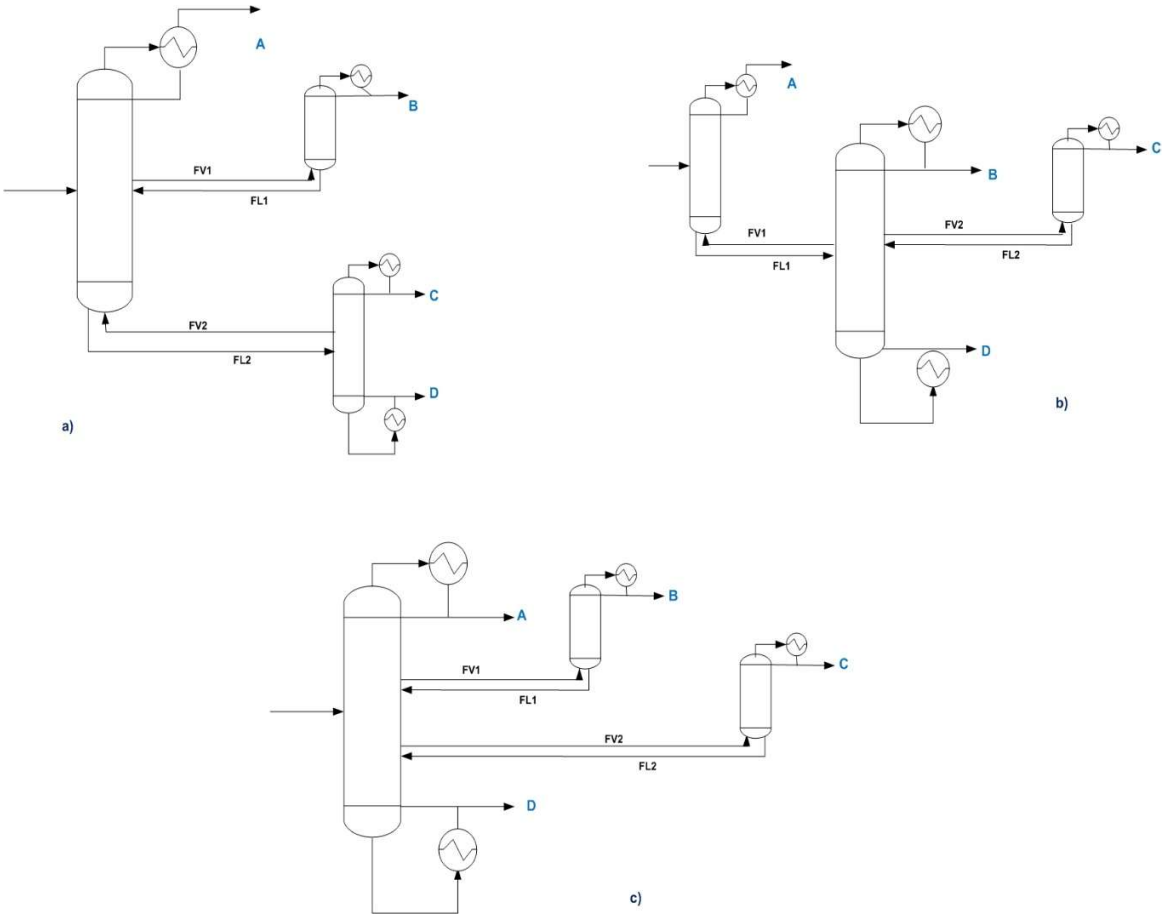

Figure 5. TES´s configurations: a) TES-1, b) TES-2, c) TES-3.

Table 7. Results of TES´s configurations.

		TES-1		
	Column 1	**Lateral section**	**Column 3**	**TOTAL**
Number of stages	32	17	87	136
Condenser duty (kW)	9,433.53	6,749.74	12,532.70	28,715.98
Reboiler Duty (kW)	0	0	34,000.64	34,000.64
		TES-2		

	Column 1	Lateral section	Column 3	TOTAL
Number of stages	16	76	44	136
Condenser duty (kW)	5,834.71	6,678.71	14,175.54	26,688.96
Reboiler Duty (kW)	0	32,000.79	0	32,002.79

TES-3

	Column 1	Lateral section	Column 3	TOTAL
Number of stages	75	17	44	136
Condenser duty (kW)	9,249.81	6,819.14	12,039.61	30,108.56
Reboiler Duty (kW)	35,393.92	0	0	35,393.92

Based on the results presented in Table 7, the sequence with lower energy consumption is TES-2, regarding TES-1 (condenser duty, 7.06% less, reboiler duty, 5.88% less) and TES-3 (condenser duty, 11.36% less, reboiler duty, 9.58% less). The ISC´s designs must be constructed based on the TES-3 structure. However, this distillation train does not have lateral transport sections; thus, ISC´s trains cannot be constructed, and the methodology ends with TES´s. Therefore, it is important to note that the energy requirements for OTC-3 are less than for TES-2: condenser duty, 21.9% less; reboiler duty, 18.3%; thereby, the OTC-3 is the train with the lowest energy consumption. Thus, the energy integration network is constructed for the process with the OTC-3 sequence. It is important to remark that all distillations sequences presented in this work have been designed to reach 99% of recovery regarding to key compounds. Likewise, a sensibility analysis was applied on each design with the objective of minimizing the reboiler duty; for this, the number of stages, the location of feed stage along with the interconnection flow rates are manipulated.

To apply the pinch point methodology, 10 streams were considered: 6 hot streams and 4 cold streams of the ATJ process with the OTC-3 sequence, whose data is presented in Table 8. The minimum

difference of temperature was chosen as 10 °C. The identification of the streams was presented in Figure 2, from section 2. The selected distillation train is shown in Figure 4.

Table 8. Streams data for pinch point methodology.

ID stream	Equipment	T in (°C)	T out (°C)	WCp (kW/°C)
H1	B1	28	21.277	231.46
C1	EX-1	21.49	360	333.12
H2	B4-CONDENSER	37.20	-218.43	2,185.23
C2	REBOILER-B4	94.91	133.99	5,953.04
H3	EX-2	148.81	120	89.10
C3	EX-3	-228.267	100	164.72
H4	COL1-CONDENSER	0.28	-0.94	4,823.76
H5	COL2-CONDENSER	69.55	67.01	1,922.39
H6	COL3-CONDENSER	212.99	141.51	140.79
C4	COL3-REBOILER	350.21	354.20	6,555.55

*H= hot stream; C= cold stream.

The application of the pinch point methodology allows to determine the cold and hot pinch point temperatures as 27.20°C and 37.20°C, respectively. Likewise, the calculated minimum heating and cooling external requirements are 364,146.38 kW and 522,072.31 kW, respectively. If these energetic requirements are compared with those required from the ATJ conventional process (Figure 2), 34.75% and 30.32% of savings are obtained for heating and cooling, respectively.

In Figure 6, the energy integration network is showed, using the nomenclature for hot and cold streams. This network was constructed considering the minimum number of heat exchangers (see Section 3), which are 7 above and 5 below the pinch point. In Figure 7, the flowsheet of the ATJ

process resulting from the application of the intensification and the energy integration strategies is presented.

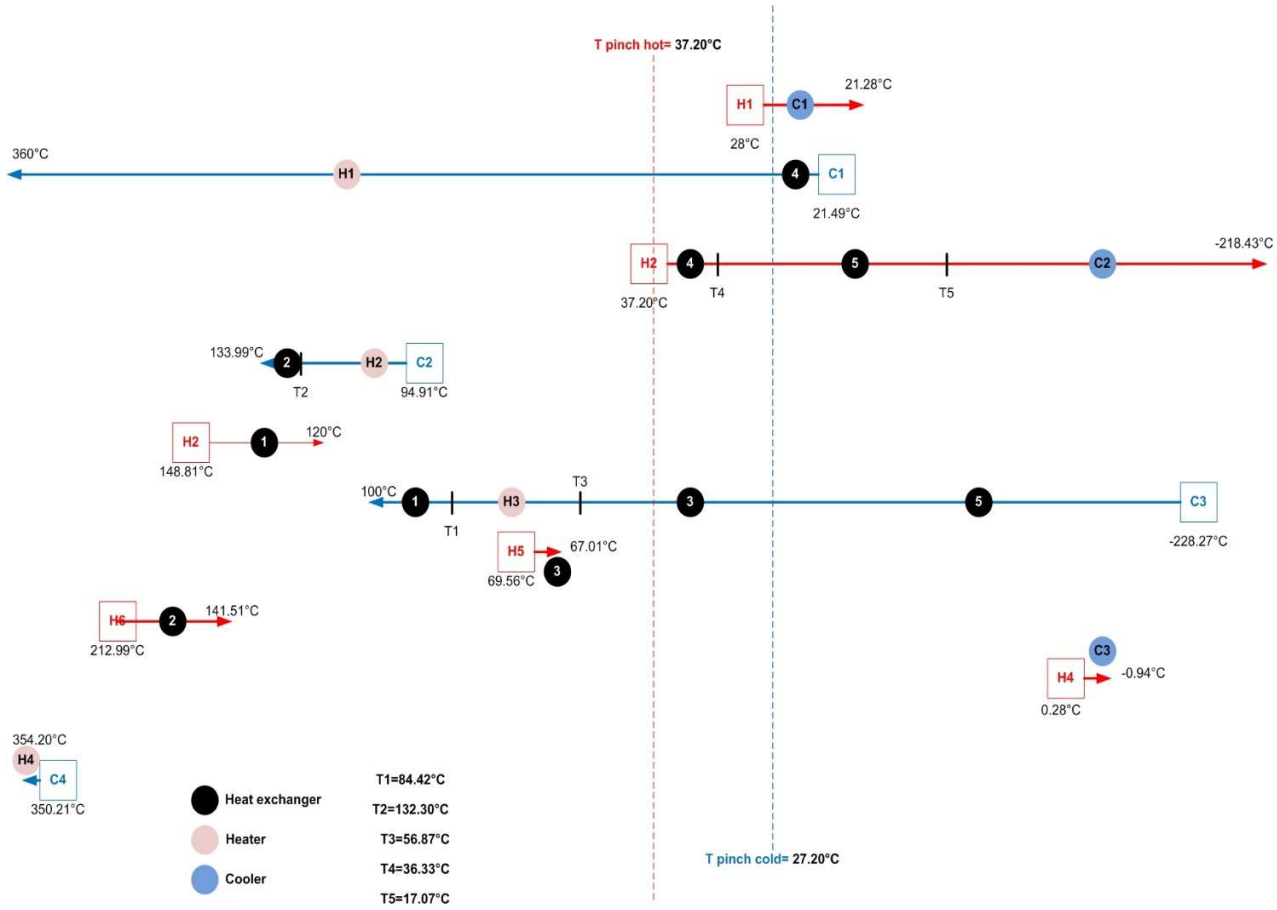

Figure 6. Energy integration network.

The results of the economic evaluation (TAC) of ATJ processes, conventional and intensified-integrated, are presented in Table 9. As it can be observed, the ATJ conventional process has the major TAC, which is 4.84% more than the intensified process. If the conventional ATJ process is compared with that reported by Tao et al. [18], the computed operating costs are 1.56 USD and 1.23 USD per each kg of biojet fuel obtained, respectively. As result of the application of process intensification and energy integration tools elevated economic savings are obtained; the steam and cooling water costs are 66.90% and 51.74% less, respectively, in comparison with the proposed conventional process. In the intensified process, note that the electricity cost is negative due to the

use of electrical energy provided by the turbines of the process. In the case of conventional process, the use of electricity from the turbines is not integrated; thus, external electricity must be provided. On the other hand, the equipment cost is higher in the intensified process, 3.15% more than conventional process; this is due to the need of additional heat exchangers in the energy integration network.

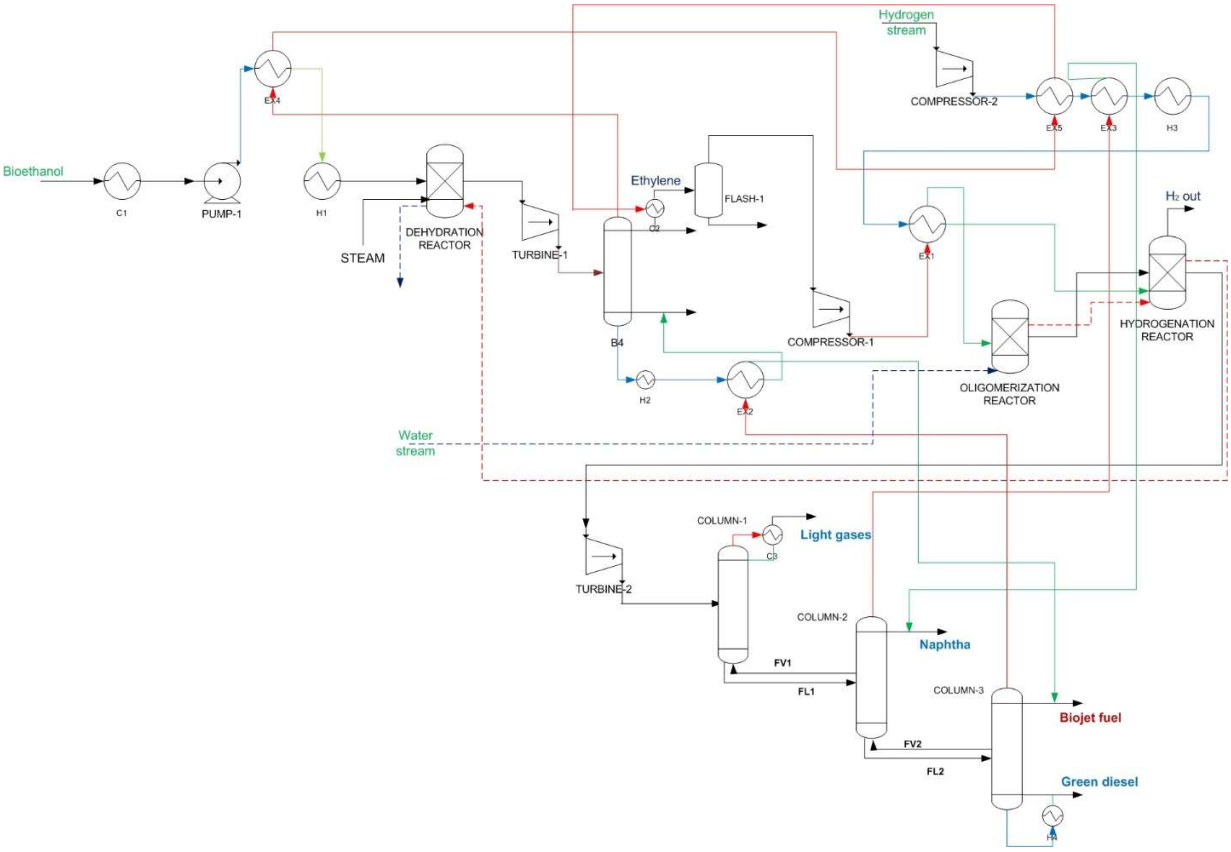

Figure 7. Flowsheet of ATJ intensified process.

Table 9. TAC for conventional and intensified ATJ process.

Costs (USD/year)	ATJ Conventional process	ATJ Intensified-integrated process
Equipment	10,821,331.67	11,162,469.87
Raw material	695,637,942.00	695,637,942.00
Steam	17,077,425.38	5,652,577.26
Cooling water	132,338.43	63,865.24
Electricity	10,320,078.11	- 13,960,955.38
Refrigerant	118,236.45	108,777.53
TAC	**734,107,352.04**	**698,664,676.52**

The results from the estimation of CO_2 emissions, derived from steam and electricity requirements, for both ATJ processes are presented in Table 10. According to results, the CO_2 emissions due to steam are 4.98% higher for conventional process, regarding the intensified process. Also, the use of generated electricity by turbines in the intensified process allows to save roughly 30,900 Ton CO_2 per year. Thereby, the use of intensified tools has a positive environmental effect.

Table 10. Estimation of CO_2 emissions for conventional and intensified ATJ processes.

CO_2 emissions (ton/year)	ATJ Conventional process	ATJ Intensified-integrated process
Steam	1,125,962.97	1,069,852.90
Electricity	22,841.77	-30,900.25
Total	**1,125,985,812.36**	**1,069,822,002.93**

Finally, Table 11 shows the results of the proposed indicators for intensified and conventional ATJ process. In the case of IE for conventional process, 6.60 kW are invested inside the process per kW released by the products. This value is high compared with the value of 4.30 for intensified process; this means that the use of intensification tools improves the energetic efficiency of the process. On the other hand, in the case of IACO2 the effect of intensified tools is notable again. This indicator means that 0.85 and 0.81 ton CO_2 are released to the atmosphere per kg of obtained products for conventional and intensified processes, respectively. Thus, the reduction of heating utilities by the intensification in the separation zone, and the use of minimum external heating services provided by the energy integration network have a significant reduction in CO_2 emissions. Likewise, the use of generated electricity provided by turbines to cover the power requirements reduced CO_2 emissions.

Table 11. Proposed indicators for conventional and intensified ATJ process.

	ATJ Conventional process	**ATJ Intensified-integrated process**
IE (kW/kW)	6.60	4.30
IACO2 (Ton CO_2/ kg)	0.85	0.81

For the intensified ATJ process, the estimation of biojet fuel minimum selling price is 0.59 USD/kg, according to the methodology proposed by [42, 49]; on the other hand, the fossil jet fuel price in the market is 0.34 USD/kg [50]. This means that the biojet fuel minimum selling price is 41.7% higher than fossil jet fuel in the market. Therefore, in order to decrease the price of biojet fuel prize it is necessary to reduce of bioethanol cost (improvement its production process), recycling the hydrogen stream, and the incorporation of the intensified ATJ process into a biorefinery scheme.

7. Conclusions

The modelling and simulation of the ATJ process to produce biojet fuel have been presented. Also, the tools of process intensification and energy integration have been applied to improve the energetic efficiency of the process, reducing the TAC and the released CO_2 emissions. The comparison between the assessment of ATJ processes, conventional and intensified-integrated, has been done through indicators. Based on the results, 21% biojet fuel yield was reached at the end of the process. Also, the use of OTC-3 allows saving 5.31% of energy at the reboiler zone, regarding the direct conventional sequence. Likewise, with the application of energy integration, 34.75% and 30.32% of heating and cooling savings are reached. Regarding the TAC evaluation, the intensified-integrated ATJ process is 4.83% less than the ATJ conventional process. In relation to CO_2 emissions, the effect of applying intensified tools is notable; the intensified-integrated process has a reduction of 4.98% for the CO_2 emissions, in comparison with the conventional process. Finally, the proposed indicators reveal that the use of process intensification and energy integration tools improve the TAC, the CO_2 emissions released, and the energetic efficiency of the process, which would enhance the economic and environmental feasibility of biojet fuel.

Acknowledgements

Financial support provided by CONACyT, grant 239765, for the development of this project is gratefully acknowledged. Also, A.G. Romero-Izquierdo was supported by a scholarship from CONACYT for the realization of her graduate studies.

Conflict of Interest

The authors declare that there is not any conflict of interest.

References

[1] BP, BP Energy Outlook, 2019 Edition. https://www.bp.com/content/dam/bp/business-sites/en/global/corporate/pdfs/energy-economics/energy-outlook/bp-energy-outlook-2019.pdf (accessed 31 July 2020).

[2] Wei, H., Liu, W., Chen, X., Yang, Q., Li, J., Chen, H., Renewable bio-jet fuel production for aviation: a review, Fuel, 254 (2019), 115599.

[3] Martinez-Hernandez, E., Ramírez-Verduzco, L.F., Amezcua-Allieri, M.A., Aburto, J., Process simulation and techno-economic analysis of bio-jet fuel and green diesel production — Minimum selling prices, Chem. Eng. Res. Des., 146 (2019), 60–70.

[4] WEF, World Economic Forum, Sustainable development impact summit. https;//weforum.org/agenda/2020/06/4-charts-airline-crisis-covid-way-ahead/ (accessed 20 September 2020].

[5] IATA, IATA Calls for passenger face covering and crew masks. http://iata.org/en/pressroom/pr/2020-05-05-01/ (accessed 20 September 2020).

[6] Gutiérrez-Antonio, C., Romero-Izquierdo, A.G., Gómez-Castro, F.I., Hernández, S., Energy integration of a hydrotreatment process for sustainable biojet fuel production, Ind. Eng. Chem. Res., 55 (2016), 8165–8175.

[7] IATA, A global approach to reducing aviation emissions from ... - Air France. https://www.yumpu.com/en/document/view/24408947/a-global-approach-to-reducing-aviation-emissions-from-air-france (accessed 30 july 2020).

[8] Gutiérrez-Antonio, C., Romero-Izquierdo, A. G., Gómez-Castro, F. I., Hernández, S., Briones-Ramírez, A., Simultaneous energy integration and intensification of the hydrotreating process to produce biojet fuel from jatropha curcas, Chem. Eng. Process.

Process Intensif., 110 (2016), 134–145.

[9] Romero-Izquierdo, A.G., Gutiérrez-Antonio, C., Gómez-Castro, F.I., Hernández, S., Hydrotreating of triglyceride feedstock to produce renewable aviation fuel, Recent Innov. Chem. Eng., 11 (2018), 77–89.

[10] Liu, G., Yan, B., Chen, G., Technical review on jet fuel production, Renew. Sustain. Energy Rev., 25 (2013), 59–70.

[11] ASTM International, ASTM D7566-19, Standard Specification for Aviation Turbine Fuel Containinf Synthesized Hydrocarbons. https://www.astm.org (accessed 25 September 2020).

[12] Gutiérrez-Antonio, C. , Romero-Izquierdo, A.G., Gómez-Castro, F.I., Hernández, S., Production Processes of Renewable Aviation Fuel, first ed., Elsevier, Amsterdam, 2021.

[13] Thion, S., Flying green sustainable aviation fuels - offseting the environmental impact of a fast growing industry. https://www.irena.org/-/media/Files/IRENA/Agency/Events/2019/May/biojet-EUBCE/5-Sthepane-Thion.pdf?la=en&hash=D11D36850F29EA282D63ECDF9B122CDFEAA7AE26 (accessed 31 July 2020)

[14] Wang, W.-C., Tao, L., Bio-jet fuel conversion technologies, Renew. Sustain. Energy Rev., 53 (2016), 801–822.

[15] CAAFI, Fuel Qualification. http://www.caafi.org/focus_areas/fuel_qualification.html (accessed 04 December 2020).

[16] IATA, Sustainable aviation fuel: technical certification. https://www.iata.org/contentassets/d13875e9ed784f75bac90f000760e998/saf-technical-certifications.pdf (accessed 04 December 2020)

[17] Atsonios, K., Kougioumtzis, M.-A., Panopoulos, K. D., Kakaras, E., Alternative

thermochemical routes for aviation biofuels via alcohols synthesis: Process modeling, techno-economic assessment and comparison, Appl. Energy, 138 (2015), 346–366.

[18] Tao, L., Markham, J. N., Haq, Z., Biddy, M. J., Techno-economic analysis for upgrading the biomass-derived ethanol-to-jet blendstocks, Green Chem. 19 (2017), 1082–1101.

[19] U. Neuling and M. Kaltschmitt, "Techno-economic and environmental analysis of aviation biofuels," *Fuel Process. Technol.*, vol. 171, pp. 54–69, 2018.

[20] S. Geleynse, Z. Jiang, K. Brandt, M. Garcia-Perez, M. Wolcott, and X. Zhang, "Pulp mill integration with alcohol-to-jet conversion technology," *Fuel Process. Technol.*, vol. 201, p. 106338, 2020.

[21] Li, H., Wu, Y., Li, X., Gao, X., State-of-the-art of advances distillation technologies in China, Chem. Eng. Technol. 39 (2016), 815-833.

[22] Gao, X., Wang, F., Li, H., Li, X., Heat-integrated reactive distillation process for TAME synthesis, Sep. and Pur. Technol. 132 (2014), 468-478.

[23] Cong, H., Li, X., Li, H., Murphy, J.P., Gao, X., Performance analysis and structural optimization of multi-tube type heat integrated distillation column (HIDiC), Sep. and Pur. Technol., 188 (2017), 303-315.

[24] Cong, H., Murphy, J.P., Li, X., Li, H., Gao, X., Feasibility evaluation of a novel middle vapor recompression distillation column, Ind. Eng. Chem. Res., 57 (2018), 6317-6329.

[25] Li, X., Cui, C., Li, H., Gao, X., Process synthesis and simultaneous optimization of extractve distillation system integrated with organic Rankine cycle and economizer for waste heat recovery, Jour. Taiwan Inst. Chem. Eng., 102 (2019), 61-72.

[26] Gutiérrez-Antonio, C., Gómez-Castro, F. I., Hernández, S., Briones-Ramírez, A., Intensification of a hydrotreating process to produce biojet fuel using thermally coupled

distillation, Chem. Eng. Process. Process Intensif. 88 (2015), 29–36.

[27] Gutiérrez-Antonio, C., Soria Ornelas, M.L., Gómez-Castro, F.I., Hernández, S., Intensification of the hydrotreating process to produce renewable aviation fuel through reactive distillation, Chem. Eng. Process. - Process Intensif. 124 (2018), 122–130.

[28] Gutiérrez-Antonio, C., Gómez-de-la-Cruz, A., Romero-Izquierdo, A.G., Gómez-Castro, F.I., Hernández, S., Modelling, simulation and intensification of hydroprocessing of micro-algae oil to produce renewable aviation fuel, Clean Technol. Envirnom. Pol., 20 (2018), 1589-1598.

[29] Gutiérrez-Antonio, C., Gómez-Castro, F.I., Hernández, S., Sustainable production of renewable aviation fuel through intensification strategies, Chem. Eng. Transac., 69 (2018), 1-6.

[30] García-Sánchez, M., Sales-Cruz, M., López-Arenas, T., Viveros-García, T., Pérez-Cisneros, E. S., An intensified reactive separation process for bio-jet diesel production, Processes, 7 (2019), 1-17.

[31] Villegas-Herrera, L.A., Gómez-Castro, F.I., Romero-Izquierdo, A.G., Gutiérrez-Antonio, C., Hernández, S., Feasibility of energy integration for high-pressure biofuels production processes, Computer Aided Chemical Engineering. 43 (2018), 1523–1528.

[32] Conde-Mejía, C., Jiménez-Gutierrez, A., El-Halwagi, M.M., Assessment of combiations between pretreatment and conversion configurations for bioethanol production, Sustainable Chemistry and Engineering, 1 (2013), 956-965.

[33] Arvidsson, M., Lundin, B., Process Integration Study of a Biorefinery Producing Ethylene from Lignocellulosic Feedstock for a Chemical Cluster, Master Thesis, Chalmers University, Göteborg, 2011.

[34] Heveling, J., Nicolaides, C.P., Scurrell, M.S., Catalysts and conditions for the highly efficient, selective and stable heterogeneous oligomerisation of ethylene, Appl. Catal. A Gen. 173 (1998), 1–9.

[35] Moussa, S., Arribas, M.A., Concepción, P., Martínez, A., Heterogeneous oligomerization of ethylene to liquids on bifunctional Ni-based catalysts: The influence of support properties on nickel speciation and catalytic performance, Catal. Today. 277 (2016), 78–88.

[36] Carlson, E.C., Don´t gamble with physical properties for simulations, Chem. Eng. Prog., 1 (1996), 35-46.

[37] Rong. B.-G., Errico, M., Synthesis of intensified simple column configurations for multicomponent distillations, Chem. Eng. Process. Process Intensif. 62 (2012), 1–17.

[38] Kemp, I., Pinch Analysis and Process Integration - A User Guide on Process Integration for the Efficiente Use of Energy, second ed., Elsevier, Amsterdam, 2006.

[39] Turton, R., Bailie, R.C., Whiting, W. B., Shaeiwitz, J. A., Bhattacharyya, D., Analysis, Synthesis, and Design of Chemical Processes, fourth ed., Prentince Hall, 2012.

[40] Luyben, M. I., Luyben, W. L., Design and control of a complex process involving two reaction steps, three distillation columns, and two recyle streams, In. Eng. Chem. Res., 34 (1995), 3885-3898.

[41] Gómez-Castro, F.., Segovia-Hernández, J.G., Hernández, S., Rico-Ramírez, V., Gutiérrez-Antonio, C., Briones-Ramírez, A., Cano-Rodríguez, I., Gamiño-Arroyo, Z., Analysis of alternative non-catalytic process for the production of biodiesle fuel, Clean Technol. Environm. Pol., 17 (2015), 2041-2054.

[42] Jiménez-Gutiérrez, A., Diseño de procesos en ingeniería química, Ed. Reverté, 2003.

[43] Mereti, Gas refrigerante. https://mereti.com.mx/categoria-producto/gas-refrigerante-2/.

(accessed 30 July 2020).

[44] Global Petrol Prices, Ethanol prices around the world. https://www.globalpetrolprices.com/ethanol_prices/ (accessed 30 july 2020).

[45] Hydrogen Energy Systems, Hydrogen Fuel Cost vs Gasoline. https://heshydrogen.com/hydrogen-fuel-cost-vs-gasoline/ (accessed 22 August 2019).

[46] CFE México, Tarifas - CFE. https://app.cfe.mx/Aplicaciones/CCFE/Tarifas/Tarifas/tarifas_industria.asp (accessed 25 August 2019).

[47] Comisión Reguladora de Energía, Factor de emisión del sector eléctrico nacional. https://www.gob.mx/cms/uploads/attachment/file/304573/Factor_de_Emisi_n_del_Sector_El_ctrico_Nacional_1.pdf (accessed 30 July 2020).

[48] Curzons, A. D., Constable, D. J. C., Mortimer, D. N., Cunningham, V. L., So you think your process is green, how do you know? - Using principles of sustainability to determine what is green - A corporate perspective, *Green Chemistry*, 3 (2001) 1–6.

[49] Martínez-Hernández, E., Ramírez-Verduzco, L.F., Amezcua-Allieri, M. A., Aburto, J., Process simulation and techno-economic analysis of bio-jet fuel and green diesel production-Minimum selling prices, *Chemical Engineering Research and Design,* 146 (2019), 60-70.

[50] Index mundi, Jet fuel daily price. https://www.indexmundi.com/commodities/?commodity=jet-fuel (accessed 12 November 2020).